Subseasonal variability of the winter North Atlantic jet stream has decreased due to climate change

communications earth & environment

Article

A Nature Portfolio journal

https://doi.org/10.1038/s43247-026-03423-0

Subseasonal variability of the winter North Atlantic jet stream has decreased due to climate change

Andrea Vito Vacca [1,2,3] ✉, Jacob Perez[4], Katinka Bellomo [5], Júlia Casadevall Díaz[3], Ieuan Davies[3], Jost von Hardenberg [1,6] & Amanda C. Maycock [3]

The North Atlantic eddy-driven jet plays a vital role in shaping Euro-Atlantic weather and climate. While previous research has focused on the seasonal mean jet response to climate change, its changes at subseasonal timescales remain poorly understood, despite the importance for extreme weather. Here, we show that over the past 75 years, wintertime subseasonal variability in jet latitude and tilt has declined by 18% and 14%, respectively. The decreased jet variability is connected to regional storm tracks, atmospheric blocking, precipitation and temperature variability in Europe. Climate models show that part of the reduction in jet variability is due to external forcing, though they tend to underestimate its magnitude. Models project that jet variability will continue to decrease throughout the 21st century under increasing global warming. These findings reveal a robust response of the North Atlantic jet to climate change with implications for current and future European weather.

Climate in the Euro-Atlantic region is strongly shaped by the North Atlantic large-scale atmospheric circulation[1–3]. Of central importance is the eddy-driven jet stream (hereafter jet), a band of strong westerly winds extending across the North Atlantic basin. The jet steers North Atlantic extratropical cyclones and, through this, plays a central role in shaping European weather and climate[4,5]. The jet dynamics are closely linked to large-scale modes of variability, such as the North Atlantic Oscillation (NAO)[6–8], along with key dynamical processes including Rossby wave breaking[9,10] and impactful phenomena like atmospheric blocking[11,12].

Most studies examining the jet response to climate change have focused on seasonal-mean or longer timescales. For instance, a recent study showed that the winter mean jet has strengthened since 1950 and that this trend is underestimated in climate models[13]. Moreover, climate change projections show large inter-model disagreement regarding winter mean trends in the jet[14–18], which undermines confidence in future climate hazards across the Euro-Atlantic region[14,19–21].

In contrast, changes in jet behaviour at shorter timescales have received less attention[22], despite the primary role of high-frequency jet fluctuations in driving extreme weather events[23,24]. For example, anomalously wide latitudinal shifts of the jet have been invoked to explain European drought conditions in 2016/2017[25], while an exceptionally strong and latitudinally steady jet has been linked with extreme cold events in 2009/10[26,27] and severe European flooding in 2013/14[28–30]. A few studies have examined changes in daily jet waviness[23,31,32], but varying definitions of waviness lead to contradictory results and complicate their interpretation[33]. The recent development of novel multi-parametric jet diagnostics has revealed new insights into the diversity of jet configurations[34–36] and their surface climate signatures[37–39]. Notably, the jet inclination (i.e., tilt) has emerged as a key parameter linked to surface weather and climate extremes[37,39,40]. However, one outstanding gap is how climate change is altering jet variability at subseasonal scales, which is the focus of the present study.

We analyse past and future subseasonal jet variability (hereafter variability) using a novel diagnostic framework (see Methods). We present here the evidence that there has been a significant decline in winter jet latitude and tilt variability over the past 75 years in observation-based reanalysis datasets. Reduced variability in jet latitude and tilt means the jet undergoes fewer meridional excursions and smaller changes in inclination within a single winter season, which we show has significant implications for European winter weather. Moreover, we show that while climate models generally underestimate the decline in latitude and tilt variability over recent decades, they consistently project a decrease in future variability under continued global warming. This suggests that the trend in reanalysis is at least partly driven by human-caused climate change and may be expected to continue in the future unless strong mitigation is achieved.

[1]Department of Environment, Land, and Infrastructure Engineering, Politecnico di Torino, Turin, Italy. [2]Istituto Universitario di Studi Superiori (IUSS Pavia), Pavia, Italy. [3]School of Earth and Environment, University of Leeds, Leeds, UK. [4]Centre for Doctoral Training in Fluid Dynamics, University of Leeds, Leeds, UK. [5]Department of Geoscience, Universitá di Padova, Padua, Italy. [6]Institute of Atmospheric Sciences and Climate, Consiglio Nazionale delle Ricerche (CNR-ISAC), Turin, Italy. ✉e-mail: andrea.vacca@polito.it

Results

Variability of the North Atlantic winter jet has declined since 1950

We begin by analysing the variability of the North Atlantic jet during winter (December-February, DJF) using the ERA5 reanalysis dataset European Centre for Medium-Range Weather Forecasts[41], over the period 1950/1951 to 2024/2025 (hereafter 1950–2024). We use a feature-extraction methodology applied to daily 850 hPa wind fields (see Methods) to analyse the time evolution of the jet latitude, tilt, and speed variability (Fig. 1, see Methods).

The jet latitude variability exhibits pronounced multi-decadal fluctuations, consistent with previous studies highlighting low-frequency variability in North Atlantic atmospheric circulation[13,42]. Superposed on these fluctuations is a long-term decrease in jet latitude variability (−0.19° decade^{-1}), which corresponds to an 18% decrease over the period 1950–2024. Jet tilt variability also shows a decreasing trend (−0.21° decade^{-1}), which corresponds to a 14% reduction over the same period. In contrast, jet speed variability does not show a significant long-term change on top of the multi-decadal variability. The trends in jet variability in ERA5 are consistent with those found in other reanalysis datasets, even if they show less statistical significance (Supplementary Fig. S4). Similar significant trends are also found using data from the backward extension of ERA5 since 1940.

Implications of declining North Atlantic jet variability

While well-known relationships exist between surface climate variables and jet characteristics at seasonal or longer timescales, we now investigate the climatic impacts of the decrease in jet variability observed in the reanalysis. We composite winters with low (below 20th percentile) and high (above 80th percentile) jet latitude variability for key diagnostics related to synoptic timescale atmospheric and surface variability: daily precipitation and temperature variability, storm track activity and atmospheric blocking frequency (Fig. 2). The differences in these diagnostics between low and high variability winters are then linearly scaled to match the 18% reduction in jet latitude variability from 1950 to 2024 (see Methods), thus providing an estimate of the climate implications resulting from this observed decrease. Notably, among the 15 winters identified with low jet latitude variability, ~75% (11 winters) occur in the latter half of the record (1988–2024), compared to only ~25% (4 winters) in the previous period (1950–1987), indicating that they are becoming more frequent given the long-term decline.

Winters featuring low jet latitude variability are associated with enhanced precipitation variability over Northern Europe, and reduced precipitation variability over Southern Europe and Greenland (Fig. 2a). This results in an enhancement of precipitation wet extremes over Northern Europe (Supplementary Fig. S5c), with changes that exceed those of the seasonal mean (Supplementary Fig. S5a). These larger responses in the tail of the distribution show that variability changes (Fig. 2a) amplify extreme precipitation beyond a simple uniform shift of the distribution. Winters with low latitude variability also exhibit lower surface temperature variability across Europe, particularly in northern regions (Fig. 2b). Cold temperature extremes are similarly reduced (Supplementary Fig. S5d). However, in this case, the change in extremes is mainly driven by changes in the seasonal-mean temperature, which is increased in low jet variability years (Supplementary Fig. S5b).

Furthermore, winters with low jet latitude variability show an intensified storm track, especially near its core and downstream sectors (Fig. 2c), and a significant decrease in atmospheric blocking especially over Greenland, the UK and Scandinavia (Fig. 2d). The intensification of the storm track in its core and its reduction at its flanks (Fig. 2c) is consistent with a less variable jet, which steers extratropical cyclones less towards the edges of the North Atlantic sector and more through its central part. The atmospheric and surface signals associated with reduced jet tilt variability are similar but weaker than those associated with muted latitude variability (Supplementary Fig. S6). These results show that the decrease in jet latitude and tilt variability over the past 75 years has contributed to shifts in surface climate variability.

Climate models underestimate the past decrease in North Atlantic jet stream variability

Previous studies have highlighted limitations of current climate models in reproducing observed winter average jet trends[13,43]. By applying our jet diagnostics to model simulations that offer a more detailed characterisation of climate variability compared to earlier studies[22], we assess whether state-of-art models can reproduce the observed decrease in jet latitude and tilt variability. We analyse historical initial condition large ensemble simulations from 11 models participating in the Coupled Model Intercomparison Project Phase 6 (see Table 1). We analyse the ensemble mean to isolate the forced trend for each model and compare the reanalysis data with the ensemble spread to account for a potential contribution of internal variability to the observed trend[44].

In all models, the ensemble mean trends show a decrease in jet latitude and tilt variability over 1950–2024 (Fig. 3). The trends are generally more significant in models with more ensemble members (see crossed dots in Fig. 3). Indeed, when limiting the analysis to only 5 ensemble members per model randomly selected 100 times, the significance of the ensemble mean trends decreases (not shown), reinforcing the importance of using large ensembles to detect and attribute forced signals in atmospheric variability. The model results indicate a contribution from external forcings to the decrease in jet variability found in the reanalysis. However, the magnitude of the ensemble mean trends is considerably weaker than the ERA5 trend by a factor of ~4. Moreover, in many of the models the decreases in jet latitude and tilt variability seen in ERA5 lie outside of the ensemble spread (Fig. 3).

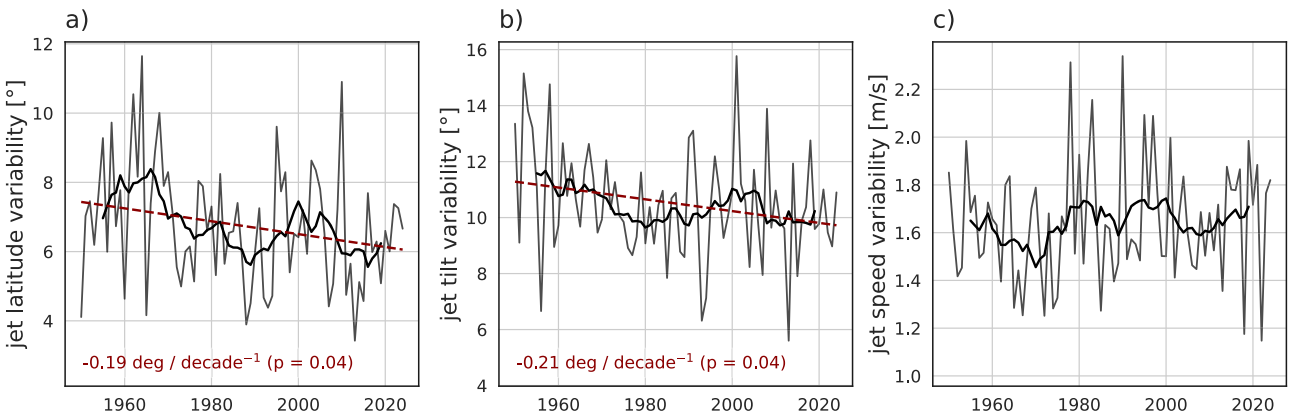

Fig. 1 | Time evolution of the North Atlantic eddy-driven jet winter variability. Timeseries (1950–2024) of the North Atlantic eddy-driven jet **a** latitude, **b** tilt, and **c** speed winter variability in the ERA5 reanalysis dataset. The thick black line represents the 11-year running mean. Red lines in (**a**) and (**b**) indicate the linear trends.

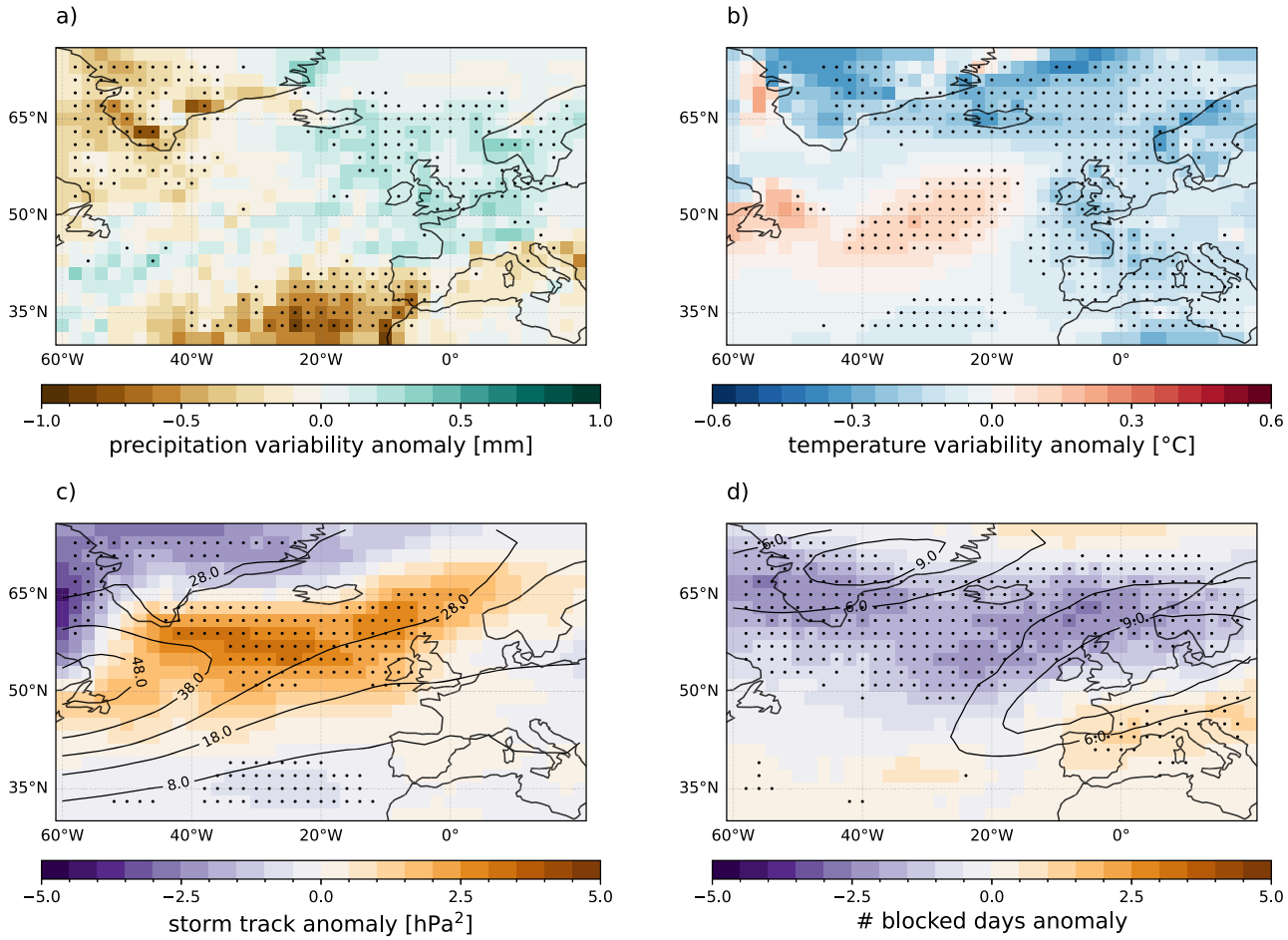

Fig. 2 | Climatic impacts of the decrease in North Atlantic eddy-driven jet latitude variability. Composite anomalies between winters with low and high North Atlantic eddy-driven jet latitude variability for **a** daily precipitation variability, **b** daily temperature variability, **c** storm track, and **d** frequency of blocked days. Variables are calculated in ERA5 reanalysis data (1950–2024). The storm track is defined as the band-pass filter (2–6 days) variance of mean sea-level pressure anomalies. The anomalies are linearly scaled to match the long-term reduction in variability over 1950–2024 (see Methods). Stippling denotes where the differences between the high and low years are statistically significant (see Methods).

Table 1 | Climate models data information

Model name	No. members	Ensemble ID
INM-CM5-0	5	`r[1-5]i1p1f1`
MRI-ESM2-0[a]	5	`r[1-5]i1p1f1`
CNRM-CM6-1	6	`r[1-6]i1p1f2`
MPI-ESM1-2-HR	10	`r[1-10]i1p1f1`
IPSL-CM6A-LR	11	`r[1-10,14]i1p1f1`
UKESM1-0-LL	14	`r[1-4,8-12,15-19]i1p1f1`
CanESM5	20	`r[1-10]i1p1f1,r[1-10]i1p1f2`
ACCESS-ESM1-5[a]	30	`r[11-40]i1p1f1`
MPI-ESM1-2-LR	50	`r[1-50]i1p1f1`
CESM2-LE	50	`1-50`
EC-Earth3-SMHI[b]	50	`r[101-150]i1p1f1`

For each ensemble member, model timeseries are constructed by concatenating historical experiments (1850–2014) with SSP3-7.0 experiments (2015–2099).
[a]MRI-ESM2-0 and ACCESS-ESM1-5 historical data are available from 1950.
[b]EC-Earth3 SHMI historical data are only available from 1970 and consequently this model is not shown in Fig. 3.

Where the ERA5 trend is within the ensemble spread, it is consistently below the 25th percentile of modelled trends. These findings could be explained by two factors (or their combination): 1) if the change in ERA5 is primarily externally-forced, this result would indicate that the models underestimate the response to climate change (low signal-to-noise[45]); 2) another possibility is that the trends in ERA5 were partly driven by low-frequency internal variability that is underestimated by the models[46–48], resulting in a trend as large as that seen in ERA5 appearing as a rare event[49]. To further investigate this second hypothesis, we construct adjusted time series of jet latitude and tilt variability by rescaling model output to match the (generally higher) ERA5 low-frequency variance (see Supplementary Note 2). Recomputing model trends using these variance-adjusted time series results in the ERA5 trend further within the model distribution (Supplementary Fig. S8). This suggests a substantial contribution of the internal multi-decadal variability to the magnitude of the jet variability trend. However, the model ensemble means remain negative, indicating that anthropogenic climate change plays a key role in driving the variability reduction.

Climate models agree on a decrease in North Atlantic jet stream variability under future climate change

We next investigate projected changes in jet variability in a scenario that includes continued increases in greenhouse gas forcing over the 21st century reaching 867 ppm atmospheric CO_2 by 2100 (SSP3–7.0[50]). Figure 4 shows

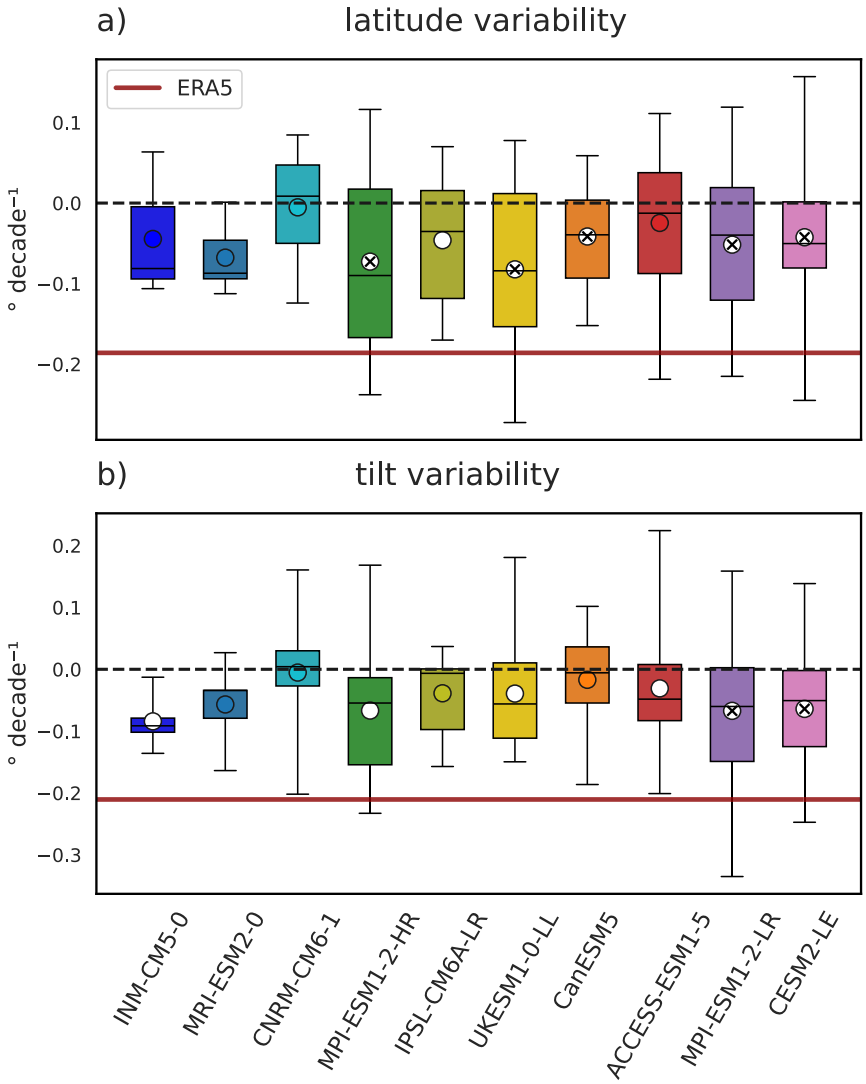

Fig. 3 | Comparison between climate models and ERA5 trends in the North Atlantic eddy-driven jet variability. Linear trends (1950–2024) in the North Atlantic eddy-driven jet variability for **a** latitude and **b** tilt computed from climate model simulations (see Methods). Box-plots represent the distribution of trends across the model ensemble members: the box spans the interquartile range (25th to 75th percentiles), the horizontal black line indicates the median, and the whiskers extend to the minimum and maximum values. Dots represent the ensemble mean trends, with their appearance denoting statistical significance: coloured dots indicate non-significant trends ($p > 0.1$), filled white dots denote significance at the 90% confidence level ($p \leq 0.1$), and white crosses denote significance at the 95% confidence level ($p \leq 0.05$). The horizontal red lines represent the ERA5 trends. Models are ordered from left to right by increasing ensemble size; only models with data available since 1950 are included (see Table 1).

the climate models consistently simulate a forced decrease in jet latitude and tilt variability over the 21st century. The magnitude of the forced decrease in latitude variability over 2025–2099 ranges from −0.05 to −0.11 ° decade^{-1} and for tilt variability −0.07 to −0.17 ° decade^{-1} (Supplementary Tables S1, S2). These trends correspond to an average future reduction in latitude and tilt variability of ~6–13% and ~5–12%, respectively, by 2099 relative to the 2024 ERA5 values (Supplementary Tables S1, S2), which would be in addition to the observed decreases of 18% and 14% between 1950 and 2024. Therefore, in a scenario without future mitigation action, the variability of the jet latitude and tilt could be lower by up to ~31% and ~26% by the end of the century compared with the mid-20th century. Moreover, this estimate could be at the lower end of what could occur, given evidence that climate models underestimate forced responses in the North Atlantic[47]. In contrast, there is no systematic projected trend in jet speed variability across the models, similar to what was seen during the recent past (Fig. 1). The consistency of the projected decrease in jet latitude and tilt variability in the models stands in stark contrast with the inconsistent seasonal mean jet trends and the NAO index, which show considerable model differences (Supplementary Note 1 and Supplementary Fig. S9), in line with previous studies[15,17,19].

Mechanism for decrease in North Atlantic jet variability

The results reveal a significant decrease in North Atlantic jet latitude and tilt variability in reanalysis data, which is simulated as an externally forced response in climate models albeit with a smaller magnitude, and is projected to continue under increasing greenhouse gas concentrations. We now seek to explain the origin of this decrease.

Some studies have suggested a relationship between the climatological jet position and its response to external forcing across climate models[15,22]. However, we find no significant relationship between the climatological seasonal jet position and the forced response in jet variability across the models (Supplementary Fig. S11). One study[22] suggested a relation between changes in jet latitude variability and seasonal mean jet shifts. However, we find no significant relationship between projected trends in seasonal mean jet latitude and the decline in variability across climate models (Supplementary Fig. S12). Another study[51] proposed that a stronger jet exhibits less latitudinal variability. This is due to the increasing Rossby wave refraction, which limits wave breaking on the poleward flank of the jet that drives jet shifting[51]. Consistent with this hypothesis, we find that at interannual timescales in ERA5 the winter jet latitude and tilt variability are anti-correlated with the seasonal mean jet speed (r = −0.55/r = −0.50, respectively; Supplementary Fig. S7). Moreover, there is a comparable correlation between the projected trends in jet latitude/tilt variability and seasonal mean jet strength, both across individual ensemble members (r = −0.44/−0.51) and the ensemble mean trends (r = −0.66/−0.62) (Fig. 5). Notably, the historical ERA5 jet latitude and tilt variability trends lie along the inter-model regression slopes (Fig. 5). We also find similar relationships between the jet latitude variability and the seasonal NAO index trends (Supplementary Fig. S10). This is expected since a more positive NAO is linked with a strengthened jet on the longer time scales[42]. These findings suggest that the

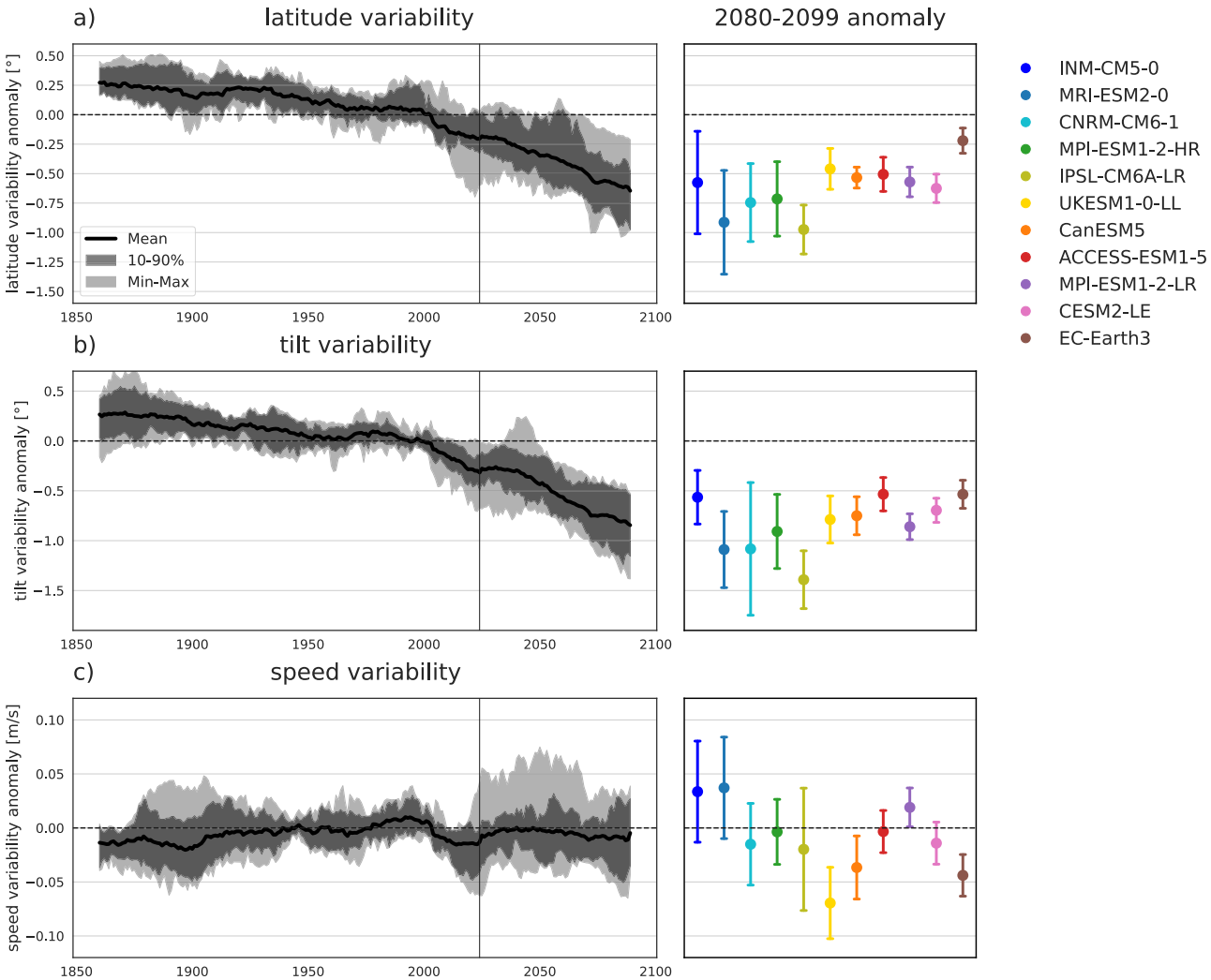

Fig. 4 | Projected evolution of the North Atlantic eddy-driven jet variability. Timeseries of North Atlantic eddy-driven jet winter variability anomaly (with respect to 1970–2014) for **a** latitude, **b** tilt and **c** speed. Solid thick lines represent the 21-year running mean multi-model average, dark shading represents 10–90th percentile range of simulations and light shading represents minimum and maximum values. The vertical line indicates the 2024 year. Right-hand panels show the anomaly in 2080–2099 with respect to 1970–2014 in individual climate models. Whiskers denote the 95% confidence interval on the mean.

decrease in jet variability in ERA5 is related to the increase in winter average jet strength and associated shift towards a more positive NAO[13]. This link is further supported by the evidence of reduced atmospheric blocking on the poleward side of the jet during years of low jet variability (Fig. 2d). Given that atmospheric blocking and Rossby wave breaking are intimately linked[11], their reduction due to a stronger jet reduces its latitudinal fluctuations, thereby reducing overall jet variability[51].

However, despite these correlations, it is important to note that the inter-ensemble and inter-model regression slopes for both jet latitude and tilt variability are offset from the origin, with the x-intercept coinciding with a negative variability trend (Fig. 5). This offset indicates that the projected changes in seasonal mean jet speed under climate change do not fully explain the modelled decline in jet variability, and suggests jet strength explains around half of the historical decrease in jet variability in ERA5.

Discussion

Our results reveal a long-term decrease in subseasonal variability of the winter North Atlantic jet latitude (18%) and tilt (13%) over the past 75 years (Fig. 1). This decline is qualitatively reproduced by climate models, although only a small number of individual ensemble members simulate a trend as large as that seen in the reanalysis datasets (Fig. 3). This suggests there is a further bias in the ability of climate models to reproduce observed North Atlantic circulation trends[13,47]. Despite this discrepancy, the ensemble mean trends consistently show a decline in jet latitude and tilt variability between 1950 and 2024, indicating an externally-forced contribution to the observed trends. The decline in subseasonal jet variability is projected to continue in a scenario with future increases in greenhouse gas concentrations (Fig. 4). In conclusion, this study reveals a robust response of the winter North Atlantic atmospheric circulation to climate change, which is already emerging in the observations. The degree of model consistency in the sign of past and future trends is remarkable for the North Atlantic atmospheric circulation, which is generally characterised by a high degree of model discrepancies[14,17]. For example, a previous study[22] found that climate models do not agree on future projections of North Atlantic jet latitude variability. However, the study used only one ensemble member per model and analyse the full year, while here we focus on the winter season and use multiple ensemble members to isolate the forced response. As we demonstrate, the inter-ensemble spread in jet variability trends is large, and the forced component is generally weak[47], so relying on a single member per model may obscure coherent forced signals.

The results showed that the ERA5 trends and the inter-model spread in the projected decreases in variability can be partly explained by changes in the winter mean jet strength (Fig. 5), which shapes the dynamics of North Atlantic Rossby wave breaking[51]. Nevertheless, the change in seasonal mean

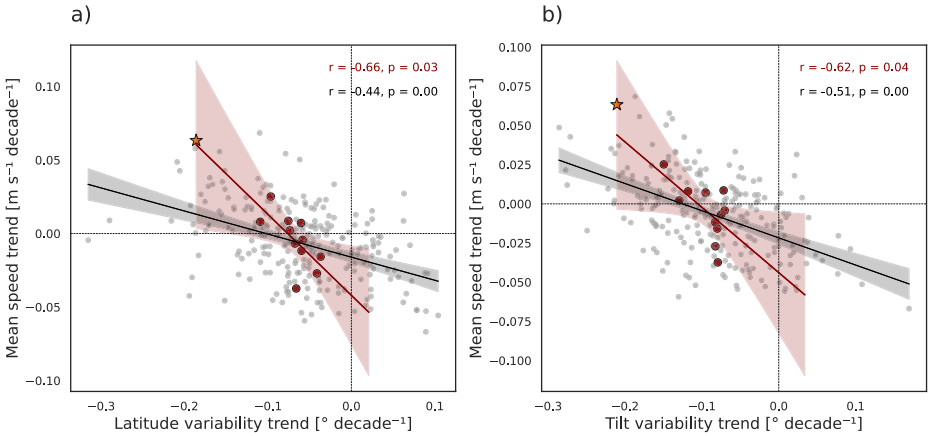

Fig. 5 | Relation between changes in the mean jet speed and changes in the jet variability. Scatterplot of 2015–2099 linear trends (SSP3–7.0) in North Atlantic eddy-driven jet winter variability of **a** latitude and **b** tilt vs. the winter mean jet speed trend. Unfilled dots represent trends in individual realizations with a linear regression in black, while filled dots represent ensemble mean trends for each model with the inter-model regression line in red. Light shading denotes the 95% uncertainty range on the regression lines. The orange stars represent linear trends in ERA5 in 1950–2024.

jet strength cannot fully explain the future change of variability (Fig. 5). We propose the decreasing jet variability could also be driven by a downstream from the North Pacific. The North Pacific jet has shifted poleward in winter over recent decades[52,53] and is simulated to continue shifting poleward in future projections under increased climate change[54]. There is evidence that this shift is linked to the Tropical Pacific sea surface temperature trends[53,55]. The North Pacific jet and storm track influence downstream development and eddy activity in the North Atlantic. At interannual timescales, when the North Pacific jet is positioned to the north, there is a greater occurrence of anticyclonic wave breaking in the North Atlantic[56–58], which is associated with weaker jet latitude variability[51]. We suggest that this non-local effect makes an additional contribution to decreased North Atlantic jet variability, alongside the local influence from changes in the seasonal mean jet strength, though this warrants further investigation.

The reduction in the meridional variability of the jet could be interpreted as a narrowing of the seasonal mean westerly flow, a feature documented in future projections[16]. However, prior assessments of jet narrowing have largely relied on multi-model ensemble means[15,59], which mask considerable inter-model spread and even divergent response signs (Supplementary Fig. S9). By contrast, the reduced subseasonal jet variability reported here emerges as a robust feature across climate models, indicating that jet narrowing and reduced jet variability are distinct and not simply two expressions of the same dynamical response. A recent study[36] has proposed that the projected mean jet narrowing arises from a blending of opposite signed externally forced mean latitudinal shifts in different winter months. We find that the projected decline in jet variability is robust in individual winter months (not shown), indicating that this mechanism cannot explain the decreases in subseasonal jet variability presented in this study. A jet exhibiting less latitudinal variability can be viewed as being closer to its climatological position, making fewer excursions to the northern and southern reaches of the North Atlantic. With this in mind, the reduced variability is in qualitative agreement with the projected increased frequency of the NAO+ weather regime[19,60,61], or relatedly the increased occurrence of the zonal geopotential jet regime[62].

The observed decrease in jet latitude variability was shown to have substantial surface impacts, including increased precipitation variability over Northern Europe and reduced variability over the Iberian Peninsula, decreased temperature variability across much of the European continent, and changes in storm track intensity and blocking frequency (Fig. 2). One study[63] identified a projected decrease in lower-tropospheric daily temperature variance in winter over northern and eastern Europe, which they linked to a shift toward less negative skewness in the temperature distribution. Our findings suggest that part of this reduction in temperature variance could be attributed to a decrease in jet variability. These impacts are likely to affect multiple socio-economic sectors, including agriculture, public health, and transportation. Moreover, since jet variability is intrinsically tied to atmospheric predictability[64–66], a reduction in variability may lead to enhanced short-term forecast skill. Thus, the projected decline in variability could have important implications for the future predictability of European winter weather.

Methods

Datasets

We use the ERA5 reanalysis dataset[41] over the period spanning from January 1950 to February 2025 (referred to as 1950–2024 winters). To check the robustness of ERA5 trends, we also use the NCAR/NCEP[67] and JRA-3Q reanalyses[68] over the same period.

We analyse 11 initial condition large ensemble simulations from the CMIP6 archive (Coupled Model Intercomparison Project phase 6), the SMHI-LENS (EC-Earth3 SMHI ensemble[69]) and the CESM2-LENS (Large-ENSemble Community program[70]), as reported in Table 1. This set of models is selected because they provide the necessary diagnostic output (i.e. daily mean zonal wind fields) for at least 5 ensemble members for both the historical and future experiments. We require these large ensembles because we are examining changes in variability, which are harder to diagnose robustly than seasonal mean changes. We use the "historical" DECK simulations covering 1850–2014[71] and the ScenarioMIP Shared Socio-Economic Pathway 3–7.0 (SSP3–7.0) experiment covering 2015–2100[50]. This scenario represents continued greenhouse gas emissions and global warming during the 21st century[14]. To calculate trends up to 2024, the historical simulations are combined with the SSP3–7.0 experiments.

Eddy-driven jet identification and diagnostics

The North Atlantic eddy-driven jet is identified starting from daily 850 hPa zonal wind fields (U850) in winter (DJF) over the North Atlantic Sector (15°–75° N, 0°–60° W), following the feature-based method presented in ref. 34. Firstly, all data are interpolated to a common 2° × 2° grid. Secondly, a low-pass Lanczos filter with a 61-day window and a 10 day cut-off frequency is applied[72] to remove short time-scale features (<10 days), and focus on the low-frequency atmospheric variability[73], though this choice does not significantly alter the daily jet statistics[34], or influence our conclusions. Hereafter, for each day, one or more Eddy-Driven Jet Objects (EDJOs) are identified in the wind field. The detection of the EDJO begins by locating the grid point with the highest U850 exceeding a certain minimum zonal wind speed threshold (U^*). For the reanalysis, $U^* = 8$ m s^{-1}[34,74], while for climate models U^* is computed as the weighted average of the climatological westerly flow. In this way, we take into account difference in models' climatologies. However, we tested the sensitivity of the results to different U^* values, finding that they are robust even with extremely conservative U^* values (i.e. U^* defined for each day as the weighted average of the westerly flow). From this grid point, all contiguous cells with U850 above the threshold are connected to delineate the extent of the EDJO. Hereafter, a minimum geodesic length requirement (L^*) is applied to retain only sufficiently zonally extended EDJOs. $L^* = 1661$ km, equivalent to the geodesic

length of the North Atlantic sector at its upper boundary (75°N). This procedure is repeated for subsequent local maxima above the threshold, enabling the identification of multiple EDJOs within the same day (see Figure 1 in Perez et al.[34], for a detailed schematic of the procedure).

Once EDJOs are identified, jet morphological features are computed using 2D spatial-moment analysis, similar to image moment analysis[75]. The moments of an EDJO are defined as:

$$M_{pq} = \int\int_{EDJO} \lambda^p \phi^q U_{850}(\lambda, \phi) dA, \quad (1)$$

where ϕ and λ are the latitude and longitude, p and q are the order of the moment in the longitudinal and latitudinal direction, and dA is the area element on a sphere. From here, the latitude of the EDJO is computed as:

$$\phi = \frac{M_{01}}{M_{00}}. \quad (2)$$

where M00 can be interpreted as the EDJO "mass". The jet speed is the average wind in the EDJO:

$$U_{\mathrm{m}} = \frac{M_{00}}{\int_{EDJO} dA}. \quad (3)$$

Finally, the tilt is the angle between the longitudinal axis and the major axis of the jet:

$$\alpha = \frac{1}{2}\arctan\left(\frac{M_{11}}{M_{20} - M_{02}}\right), \quad (4)$$

where positive values indicate a tilt from south west to north east and north west to south east for negative values. An example of the jet detection and the computation of the daily jet diagnostics is reported in the Supplementary Fig. S1.

Note that this 2D jet identification method differs from zonally-averaged approaches used in many previous studies, most notably the one-dimensional Jet Latitude Index (JLI)[74]. In contrast to the JLI, which can exhibit artefacts during periods of strong jet tilting or splitting, the methodology used here provides robust estimates of jet latitude, speed, and tilt under such complex configurations[34]. This robustness is critical for analysing subseasonal variability, which is inherently sensitive to high-frequency noise. Furthermore, the JLI produces a trimodal distribution of winter daily jet latitude, which makes the standard deviation a less robust measure of variance, while our method produces a unimodal distribution (Supplementary Fig. S2). Nevertheless, sensitivity tests applying the JLI to ERA5 data produce a negative trend in jet latitude variability consistent with our results (Supplementary Fig. S2), confirming that the decline in jet variability is not strongly sensitive to the methodology used. A detailed comparison between these methods is provided in ref. 34.

Variability diagnostic

We define the subseasonal variability of jet latitude, tilt and speed within a winter season (DJF) as the standard deviation (σ) of daily values. Since the distributions of these variables are more Gaussian than has been found for some other North Atlantic jet diagnostics[74], the standard deviation is reasonable to describe the total variability. In Fig. 2, the winter season variability of temperature and precipitation is also computed as the standard deviation of daily values for each-grid point[63,76]. In Fig. 2, the composite anomalies between low and high variability winters are scaled by a factor k in order to reflect the observed reduction in jet latitude variability. In particular,

$$k = \frac{\Delta\sigma_{obs}}{\Delta\sigma_{low-high}} = 0.3 \quad (5)$$

Where $\Delta\sigma_{obs} = -1.425°$ is the ERA5 reduction in jet latitude variability (1950–2024) and $\Delta\sigma_{low-high} = -4.75°$ is the average jet latitude variability difference between low (20th percentile) and high (above 80th percentile) variability years.

Atmospheric blocking diagnostic

To compute the atmospheric blocking frequency, we employ a two-dimensional absolute index based on the reversal of the geopotential height gradient, following the method described by Davini et al.[12]. Specifically, for each grid point, we evaluate the northward (GHGN) and southward (GHGS) gradients of the 500 hPa geopotential height:

$$GHGN(\phi_0, \lambda_0) = \frac{zg500(\phi_N, \lambda_0) - zg500(\phi_0, \lambda_0)}{\phi_N - \phi_0} \quad (6)$$

$$GHGS(\phi_0, \lambda_0) = \frac{zg500(\phi_0, \lambda_0) - zg500(\phi_0, \lambda_S)}{\phi_0 - \phi_S} \quad (7)$$

Here, λ_0 and ϕ_0 denote the longitude and latitude of the grid point, respectively, with ϕ_0 ranging from 30°N to 75°N and λ_0 from 0° to 360°. The latitudes $\phi_s = \phi_0 - 15°$ and $\phi_N = \phi_0 + 15°$ define the southern and northern reference points used in the gradient calculations. An instantaneous blocking event is identified at the grid point (λ_0, ϕ_0) if the following condition is met:

$$GHGS(\phi_0, \lambda_0) > 0; GHGN(\phi_0, \lambda_0) < -10\,\mathrm{m\,lat^{-1}} \quad (8)$$

To isolate synoptic-scale and quasi-stationary blocking events, we apply the tracking algorithm described in ref. 77, Appendix A. The algorithm filters out events with a duration shorter than 5 days or a spatial extent smaller than 500,000 km^2.

Statistical tests

We assess the significance of the long-term trends and correlations between the variables using a non-parametric bootstrap approach. Here, data points are randomly shuffled 10^4 times, and the trend slope or the correlation is recalculated at each iteration. The corresponding p-value is the fraction of bootstrap iterations in which the absolute value of the resampled slope/correlation exceeds that of the original dataset. We consider strongly statistically significant relationships with $p < 0.05$, marginally statistically significant $0.1 < p < 0.05$. To assess the statistical significance of the difference between low- and high-variability years in Fig. 2, we apply a Welch's t test at 95% confidence level[78].

Data availability

The CMIP6 model output data are publicly available at https://esgf-metagrid.cloud.dkrz.de/search/cmip6-dkrz/. The reanalysis datasets are publicly available: ERA5 from https://cds.climate.copernicus.eu/, JRA-3Q from https://rda.ucar.edu/datasets/d640000/, NCAR/NCEP from https://psl.noaa.gov/data/gridded/data.ncep.reanalysis2.html. The preprocessed data for reproducing the figures are available at: https://doi.org/10.5281/zenodo.18852321.

Code availability

The eddy-driven jet detection algorithm is available from https://github.com/scjpleeds/EDJO-identification. The atmospheric blocking algorithm is available from https://github.com/michele-filippucci/blocktrack. The code for reproducing the figures is available at: https://doi.org/10.5281/zenodo.18852321.

Received: 18 September 2025; Accepted: 10 March 2026;
Published online: 09 April 2026

References

1. Woollings, T. Dynamical influences on european climate: an uncertain future. *Philos. Trans. R. Soc. A* **368**, 3733–3756 (2010).
2. Deser, C. & Phillips, A. S. A range of outcomes: the combined effects of internal variability and anthropogenic forcing on regional climate trends over Europe. *Nonlinear Process. Geophys.* **30**, 63–84 (2023).
3. Deser, C., Knutti, R., Solomon, S. & Phillips, A. S. Communication of the role of natural variability in future North American climate. *Nat. Clim. Change* **2**, 775–779 (2012).
4. Pinto, J. G. et al. Large-scale dynamics associated with clustering of extratropical cyclones affecting Western Europe. *J. Geophys. Res.* **119**, 13,704–13,719 (2014).
5. Gaetani, M., Baldi, M., Dalu, G. A. & Maracchi, G. Jetstream and rainfall distribution in the Mediterranean region. *Nat. Hazards Earth Syst. Sci.* **11**, 2469–2481 (2011).
6. Athanasiadis, P. J., Wallace, J. M. & Wettstein, J. J. Patterns of wintertime jet stream variability and their relation to the storm tracks. *J. Atmos. Sci.* **67**, 1361–1381 (2010).
7. Benedict, J. J., Lee, S. & Feldstein, S. B. Synoptic view of the North Atlantic oscillation. *J. Atmos. Sci.* **61**, 121–144 (2004).
8. Franzke, C., Lee, S. & Feldstein, S. B. Is the North Atlantic oscillation a breaking wave?. *J. Atmos. Sci.* **61**, 145–160 (2004).
9. Tamarin-Brodsky, T. & Harnik, N. The relation between Rossby wave-breaking events and low-level weather systems. *Weather Clim. Dyn.* **5**, 87–108 (2024).
10. Barnes, E. A. & Hartmann, D. L. Rossby wave scales, propagation, and the variability of eddy-driven jets. *J. Atmos. Sci.* **68**, 2893–2908 (2011).
11. Woollings, T. et al. Blocking and its response to climate change. *Curr. Clim. Change Rep.* **4**, 287–300 (2018).
12. Davini, P., Cagnazzo, C., Gualdi, S. & Navarra, A. Bidimensional diagnostics, variability, and trends of Northern Hemisphere blocking. *J. Clim.* **25**, 6496–6509 (2012).
13. Blackport, R. & Fyfe, J. C. Climate models fail to capture strengthening wintertime North Atlantic jet and impacts on Europe. *Sci. Adv.* **8**, eabn3112 (2022).
14. Lee, J.-Y. et al. Future global climate: scenario-based projections and near-term information. In *Climate Change 2021: The Physical Science Basis. Contribution of Working Group I to the Sixth Assessment Report of the Intergovernmental Panel on Climate Change*, book section 4 (eds Masson-Delmotte, V. et al.) 553–672 (Cambridge University Press, 2021).
15. Oudar, T., Cattiaux, J. & Douville, H. Drivers of the Northern Extratropical Eddy-Driven Jet Change in CMIP5 and CMIP6 Models. *Geophys. Res. Lett.* **47**, e2019GL086695 (2020).
16. Peings, Y., Cattiaux, J., Vavrus, S. J. & Magnusdottir, G. Projected squeezing of the wintertime North-Atlantic jet. *Environ. Res. Lett.* **13**, 074016 (2018).
17. Shepherd, T. G. Atmospheric circulation as a source of uncertainty in climate change projections. *Nat. Geosci.* **7**, 703–708 (2014).
18. McKenna, C. M. & Maycock, A. C. Sources of uncertainty in multimodel large ensemble projections of the winter North Atlantic oscillation. *Geophys. Res. Lett.* **48**, e2021GL093258 (2021).
19. Vacca, A. V., Bellomo, K., Fabiano, F. & von Hardenberg, J. On the role of AMOC weakening in shaping wintertime Euro-Atlantic atmospheric circulation. *Clim. Dyn.* **63**, 273 (2025).
20. Fereday, D., Chadwick, R., Knight, J. & Scaife, A. A. Atmospheric dynamics is the largest source of uncertainty in future winter European rainfall. *J. Clim.* **31**, 963–977 (2018).
21. McKenna, C. M. & Maycock, A. C. The role of the north atlantic oscillation for projections of winter mean precipitation in europe. *Geophys. Res. Lett.* **49**, e2022GL099083 (2022).
22. Barnes, E. A. & Polvani, L. Response of the midlatitude jets, and of their variability, to increased greenhouse gases in the CMIP5 models. *J. Clim.* **26**, 7117–7135 (2013).
23. Röthlisberger, M., Pfahl, S. & Martius, O. Regional-scale jet waviness modulates the occurrence of midlatitude weather extremes. *Geophys. Res. Lett.* **43**, 10,989–10,997 (2016).
24. Mahlstein, I., Martius, O., Chevalier, C. & Ginsbourger, D. Changes in the odds of extreme events in the Atlantic basin depending on the position of the extratropical jet. *Geophys. Res. Lett.* **39,** L22805 (2012).
25. García-Herrera, R. et al. The European 2016/17 Drought. *J. Clim.* **32**, 3169–3187 (2019).
26. Santos, J. A., Woollings, T. & Pinto, J. G. Are the Winters 2010 and 2012 Archetypes Exhibiting Extreme Opposite Behavior of the North Atlantic Jet Stream?. *Monthly Weather Rev.* **141**, 3626–3640 (2013).
27. Cattiaux, J. et al. Winter 2010 in Europe: a cold extreme in a warming climate. *Geophys. Res. Lett.* **37,** L20704 (2010).
28. Rousi, E., Selten, F., Rahmstorf, S. & Coumou, D. Changes in North Atlantic atmospheric circulation in a warmer climate favor winter flooding and summer drought over Europe. *J. Clim.* **34**, 2277–2295 (2021).
29. Huntingford, C. et al. Potential influences on the United Kingdom's floods of winter 2013/14. *Nat. Clim. Change* **4**, 769–777 (2014).
30. Pall, P. et al. Anthropogenic greenhouse gas contribution to flood risk in England and Wales in autumn 2000. *Nature* **470**, 382–385 (2011).
31. Barnes, E. A. Revisiting the evidence linking arctic amplification to extreme weather in midlatitudes. *Geophys. Res. Lett.* **40**, 4734–4739 (2013).
32. Barnes, E. A. & Screen, J. A. The impact of arctic warming on the midlatitude jet-stream: can it? has it? will it?. *WIREs Clim. Change* **6**, 277–286 (2015).
33. Geen, R. et al. An explanation for the metric dependence of the midlatitude jet-waviness change in response to polar warming. *Geophys. Res. Lett.* **50**, e2023GL105132 (2023).
34. Perez, J., Maycock, A. C., Griffiths, S. D., Hardiman, S. C. & McKenna, C. M. A new characterisation of the North Atlantic eddy-driven jet using two-dimensional moment analysis. *Weather Clim. Dyn.* **5**, 1061–1078 (2024).
35. Barriopedro, D., Ayarzagüena, B., García-Burgos, M. & García-Herrera, R. A multi-parametric perspective of the North Atlantic eddy-driven jet. *Clim. Dyn.* **61**, 375–397 (2023).
36. García-Burgos, M., Ayarzagüena, B., Barriopedro, D., Woollings, T. & García-Herrera, R. Intraseasonal shift in the wintertime North Atlantic jet structure projected by CMIP6 models. *npj Clim. Atmos. Sci.* **7**, 234 (2024).
37. Galfi, V. M. & Messori, G. Erratum: Persistent anomalies of the north atlantic jet stream and associated surface extremes over europe (2023 environ. res. lett. 18 024017). *Environ. Res. Lett.* **18**, 039602 (2023).
38. Maddison, J. W., Ayarzagüena, B., Barriopedro, D. & García-Herrera, R. Added value of a multiparametric eddy-driven jet diagnostic for understanding European air stagnation. *Environ. Res. Lett.* **18**, 084022 (2023).
39. García-Burgos, M., Ayarzagüena, B., Barriopedro, D. & García-Herrera, R. Jet configurations leading to extreme winter temperatures over Europe. *J. Geophys. Res.* **128**, e2023JD039304 (2023).
40. Brönnimann, S. et al. Past hydroclimate extremes in Europe driven by Atlantic jet stream and recurrent weather patterns. *Nat. Geosci.* **18**, 246–253 (2025).
41. Hersbach, H. et al. The ERA5 global reanalysis. *Q. J. R. Meteorol. Soc.* **146**, 1999–2049 (2020).
42. Woollings, T. et al. Contrasting interannual and multidecadal NAO variability. *Clim. Dyn.* **45**, 539–556 (2015).
43. Hermoso, A., Riviére, G., Harvey, B., Methven, J. & Schemm, S. A dynamical interpretation of the intensification of the winter north atlantic jet stream in reanalysis. *J. Clim.* **37**, 5853–5881 (2024).
44. Deser, C. et al. Insights from earth system model initial-condition large ensembles and future prospects. *Nat. Clim. Change* **10**, 277–286 (2020).

45. Scaife, A. A. & Smith, D. A signal-to-noise paradox in climate science. *npj Clim. Atmos. Sci.* **1**, 1–8 (2018).
46. Bonnet, R., McKenna, C. M. & Maycock, A. C. Model spread in multidecadal North Atlantic Oscillation variability connected to stratosphere-troposphere coupling. *Weather Clim. Dyn.* **5**, 913–926 (2024).
47. Smith, D. M. et al. Mitigation needed to avoid unprecedented multi-decadal North Atlantic Oscillation magnitude. *Nat. Clim. Change* **15**, 403–410 (2025).
48. Simpson, I. R., Deser, C., McKinnon, K. A. & Barnes, E. A. Modeled and observed multidecadal variability in the North Atlantic jet stream and its connection to sea surface temperatures. *J. Clim.* **31**, 8313–8338 (2018).
49. Eade, R., Stephenson, D. B., Scaife, A. A. & Smith, D. M. Quantifying the rarity of extreme multi-decadal trends: how unusual was the late twentieth century trend in the North Atlantic Oscillation?. *Clim. Dyn.* **58**, 1555–1568 (2022).
50. O'Neill, B. C. et al. The scenario model intercomparison project (scenarioMIP) for CMIP6. *Geosci. Model Dev.* **9**, 3461–3482 (2016).
51. Woollings, T. et al. Daily to decadal modulation of jet variability. *J. Clim.* **31**, 1297–1314 (2018).
52. Keel, T., Brierley, C., Edwards, T. & Frame, T. H. A. Exploring uncertainty of trends in the North Pacific jet position. *Geophys. Res. Lett.* **51**, e2024GL109500 (2024).
53. Patterson, M. & O'Reilly, C. H. Climate models struggle to simulate observed north pacific jet trends, even accounting for tropical pacific sea surface temperature trends. *Geophys. Res. Lett.* **52**, e2024GL113561 (2025).
54. Ossó, A. et al. Advancing our understanding of eddy-driven jet stream responses to climate change–a roadmap. *Curr. Clim. Change Rep.* **11**, 2 (2024).
55. Kang, J. M., Thomas, R., Dunstone, N., Shaw, T. A. & Woollings, T. Robust impact of tropical Pacific SST trends on global and regional circulation in boreal winter. *npj Clim. Atmos. Sci.* **8**, 315 (2025).
56. Drouard, M., Riviére, G. & Arbogast, P. The link between the north pacific climate variability and the north atlantic oscillation via downstream propagation of synoptic waves. *J. Clim.* **28**, 3957–3976 (2015).
57. Li, Y. & Lau, N.-C. Impact of enso on the atmospheric variability over the north atlantic in late winter-role of transient eddies. *J. Clim.* **25**, 320–342 (2012).
58. Li, Y. & Lau, N.-C. Contributions of downstream eddy development to the teleconnection between enso and the atmospheric circulation over the north atlantic. *J. Clim.* **25**, 4993–5010 (2012).
59. Harvey, B. J., Cook, P., Shaffrey, L. C. & Schiemann, R. The response of the northern hemisphere storm tracks and jet streams to climate change in the CMIP3, CMIP5, and CMIP6 climate models. *J. Geophys. Res.* **125**, e2020JD032701 (2020).
60. Fabiano, F., Meccia, V. L., Davini, P., Ghinassi, P. & Corti, S. A regime view of future atmospheric circulation changes in northern mid-latitudes. *Weather Clim. Dyn.* **2**, 163–180 (2021).
61. Madonna, E., Li, C., Grams, C. M. & Woollings, T. The link between eddy-driven jet variability and weather regimes in the North Atlantic-European sector. *Q. J. R. Meteorol. Soc.* **143**, 2960–2972 (2017).
62. Dorrington, J., Strommen, K., Fabiano, F. & Molteni, F. CMIP6 models trend toward less persistent european blocking regimes in a warming climate. *Geophys. Res. Lett.* **49**, e2022GL100811 (2022).
63. Tamarin-Brodsky, T., Hodges, K., Hoskins, B. J. & Shepherd, T. G. Changes in northern hemisphere temperature variability shaped by regional warming patterns. *Nat. Geosci.* **13**, 414–421 (2020).
64. Franzke, C. & Woollings, T. On the persistence and predictability properties of north atlantic climate variability. *J. Clim.* **24**, 466–472 (2011).
65. Frame, T. H. A., Ambaum, M. H. P., Gray, S. L. & Methven, J. Ensemble prediction of transitions of the north atlantic eddy-driven jet. *Q. J. R. Meteorol. Soc.* **137**, 1288–1297 (2011).
66. Frame, T. H. A., Methven, J., Gray, S. L. & Ambaum, M. H. P. Flow-dependent predictability of the north atlantic jet. *Geophys. Res. Lett.* **40**, 2411–2416 (2013).
67. Slivinski, L. C. et al. Towards a more reliable historical reanalysis: Improvements for version 3 of the Twentieth Century Reanalysis system. *Q. J. R. Meteorol. Soc.* **145**, 2876–2908 (2019).
68. Kobayashi, C. & Iwasaki, T. Brewer-Dobson circulation diagnosed from JRA-55. *J. Geophys. Res. Atmos.* **121**, 1493–1510 (2016).
69. Wyser, K. et al. The SMHI Large Ensemble (SMHI-LENS) with EC-Earth3.3.1. *Geosci. Model Dev.* **14**, 4781–4796 (2021).
70. Rodgers, K. B. et al. Ubiquity of human-induced changes in climate variability. *Earth Syst. Dyn.* **12**, 1393–1411 (2021).
71. Eyring, V. et al. Overview of the coupled model intercomparison project phase 6 (CMIP6) experimental design and organization. *Geosci. Model Dev.* **9**, 1937–1958 (2016).
72. Duchon, C. E. Lanczos filtering in one and two dimensions. *J. Appl. Meteorol. Climatol.* **18**, 1016–1022 (1979).
73. Hannachi, A., Straus, D. M., Franzke, C. L. E., Corti, S. & Woollings, T. Low-frequency nonlinearity and regime behavior in the Northern Hemisphere extratropical atmosphere. *Rev. Geophys.* **55**, 199–234 (2017).
74. Woollings, T., Hannachi, A. & Hoskins, B. Variability of the North Atlantic eddy-driven jet stream. *Q. J. R. Meteorol. Soc.* **136**, 856–868 (2010).
75. Nasrudin, M. W. et al. Moment Invariants technique for image analysis and its applications: a review. *J. Phys. Conf. Ser.* **1962**, 012028 (2021).
76. Pendergrass, A. G., Knutti, R., Lehner, F., Deser, C. & Sanderson, B. M. Precipitation variability increases in a warmer climate. *Sci. Rep.* **7**, 17966 (2017).
77. Filippucci, M., Bordoni, S. & Davini, P. Impact of stochastic physics on the representation of atmospheric blocking in EC-Earth3. *Weather Clim. Dyn.* **5**, 1207–1222 (2024).
78. Welch, B. L. The generalization of 'student's' problem when several different population variances are involved. *Biometrika* **34**, 28–35 (1947).

Acknowledgements

AVV was supported by the Italian inter-university PhD course in sustainable development and climate change (link: www.phd-sdc.it). K.B. acknowledges "The Geosciences for Sustainable Development" project (Budget Ministero dell'Universitá e della Ricerca-Dipartimenti di Eccellenza 2023-2027 C93C23002690001). A.C.M. was supported by the UK Natural Environment Research Council StratClust grant (NE/X011933/1). J.P. was supported by the EPSRC Fluids Centre for Doctoral Training at the University of Leeds. I.D. was supported by a NERC PANORAMA Doctoral Training Partnership Research Experience Placement and the Leverhulme Trust. J.v.H. acknowledges funding from the European Union Next-GenerationEU within the RETURN Extended Partnership (National Recovery and Resilience Plan NRRP, Mission 4, Component 2, Investment 1.3 D.D. 1243 2/8/2022, PE0000005). We acknowledge the Coupled Modelling Working Group of the World Climate Research Programme for overseeing CMIP, the climate modelling groups for producing the model outputs, and the Earth System Grid Federation (ESGF) for enabling public access to these data.

Author contributions

A.C.M. and A.V.V. designed the study. J.P., J.C. and I.D. accessed data and performed preliminary analyses. A.V.V. performed the main analysis and produced the figures. A.C.M., J.P., K.B. and J.v.H. provided feedback on the results. A.V.V. and A.C.M. drafted the manuscript. All authors provided feedback on the manuscript.

Competing interests

The authors declare no competing interests.

Additional information

Supplementary information The online version contains supplementary material available at https://doi.org/10.1038/s43247-026-03423-0.

Correspondence and requests for materials should be addressed to Andrea Vito Vacca.

Peer review information : *Communications Earth and Environment* thanks Christian L. E. Franzke and the other, anonymous, reviewer(s) for their contribution to the peer review of this work. Primary Handling Editors: Seung-Ki Min and Alireza Bahadori. A peer review file is available.